双相钢胶焊与电阻点焊接头性能对比分析

孙海涛， 张延松， 来新民， 陈关龙
（上海交通大学 上海市数字化汽车车身工程重点实验室，上海 200240）

孙海涛

摘 要：从接头的拉剪力、熔核的微观组织、动态电阻曲线和焊接性范围 4 个方面，对比分析双相钢透胶胶焊和电阻点焊的接头性能. 结果表明，胶焊熔核开始形成时间提前于点焊，使得在小电流情况下胶焊的焊点拉剪力要普遍高于点焊；胶焊在中等电流情况下便会产生严重飞溅，使得在大电流情况下点焊焊点拉剪力要更高些. 因此，在制定胶焊的焊接工艺参数时应选择比电阻点焊偏低的焊接电流，而适度增加焊接过程的电极力有利于抑制飞溅产生.

关键词：胶焊；电阻点焊；双相钢；接头性能
中图分类号：TG455 文献标识码：A 文章编号：0253－360X(2009)10－0017－04

0 序 言

现代汽车车身的轻量化需求，使得汽车板的主要发展趋势是以双相钢为代表的先进高强度钢板的大量使用. 点焊一直以来都是车身焊接中运用最为广泛的焊接技术. 然而，在使用传统点焊焊接先进高强钢时出现了种种问题. 例如，高强钢点焊时易出现飞溅、焊接性范围较窄[1]和界面撕裂[2]等问题；还有点焊本身的缺点，如焊点处存在很大的应力集中，严重影响了焊接接头的疲劳性能. NVH(noise, vibration and harshness)技术的迅速发展和环氧基结构胶的出现，使得胶粘技术在汽车领域开始逐步获得应用. 胶粘技术具有连接处应力分布均匀、疲劳寿命增加、减重和易于任意材料和复杂结构的板材连接等特点. 但环氧基结构胶的脆性较大，在冲击载荷作用下易发生断裂失效，低温下静载强度显著下降，使得胶粘技术的普及受到了诸多限制[3].

综合以上两种连接技术的优点，出现了胶焊技术(胶粘和电阻点焊相结合的一种复合连接技术)，已经在航空航天和汽车制造等工业领域获得了广泛应用. 对于汽车制造来说，胶层的存在，克服了点焊的缺点，其应力分布均匀，疲劳强度高，减小了界面撕裂，减震能力强，无需密封工艺[4]；焊点的存在，克服了胶粘的缺点，其抗冲击能力强，低温、潮湿环境下仍有较高的静载强度[5]. 它适合于各种有机涂层或金属涂层低碳钢、高强钢、铝合金和复合材料等之间的连接.

根据工艺顺序不同，可把胶焊工艺分为两种类型：毛细作用胶焊(先点焊，后塞胶，最后固化)和透胶胶焊(先涂胶，后点焊，最后固化). 1998 年，Darwish 等人[6]研究了毛细作用胶焊(flow-in weld-bond technique)和透胶胶焊(weld-through technique)两种工艺下试样(1.5 mm 低碳钢，低聚物环氧基结构胶)的微观结构和焊接质量，提出毛细作用胶焊工艺比透胶胶焊具有更好的微观结构，且更经济. 但毛细作用胶焊技术对工艺要求高，不易实现自动化，同时由于它仅仅是点焊和胶粘技术的叠加，无法改善高强钢点焊的问题. 因此，目前透胶胶焊应用最为广泛. 但是由于钢板搭接面上绝缘胶层的存在，使得钢板间的接触状态和焊接的导电性和传热性均发生变化，因此透胶胶焊中的点焊要不同于普通点焊. 为了使透胶胶焊技术获得广泛应用，必须要深入分析胶焊接头性能相对于普通点焊的不同点.

文中从接头的拉剪强度、熔核的微观组织、动态电阻曲线和焊接性范围 4 个方面，深入对比分析双相钢透胶胶焊(以下简称胶焊)和电阻点焊的接头性能，为胶焊技术的焊接工艺参数制定提供了参考.

1 试验方法

试验采用厚度为 0.75 mm 的双相钢 DP600，属于先进高强钢，其化学成分(质量分数，%)为：C 0.106，Mn 1.53，Si 0.201，Al 0.031，Ti 0.018，S

收稿日期：2008－07－14
基金项目：国家自然科学基金资助项目(50905111)

0.001, P 0.12. 试验分别对这种钢板进行等厚钢板的胶焊和点焊, 使用相同的焊接工艺参数(表 1). 胶焊工艺中使用的胶粘剂是环氧树脂结构胶. 焊件尺寸及搭接长度见图 1.

表 1 焊接工艺参数

Table 1 Welding parameters

材料	电极力 F_1/kN	焊接电流 I/kA	焊接时间 t(周波)
0.75 mm DP600	2.2	7~12	8~12

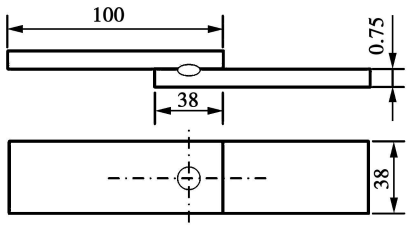

图 1 焊件尺寸及搭接长度(mm)

Fig. 1 Dimensions of weldment and overlap

胶焊的工艺方法主要有两种: 毛细作用胶焊和透胶胶焊. 前者是先点焊后塞胶最后固化胶层, 后者是先涂胶再点焊最后固化胶层. 毛细作用胶焊仅仅是点焊和胶粘的叠加, 其焊接过程与点焊一致. 目前常用的透胶胶焊, 由于在点焊之前钢板搭接面上已经有胶层, 所以其焊接过程明显不同于点焊. 在此, 为深入分析胶层对焊接强度的影响, 采用的是透胶胶焊工艺. 同时为便于对比分析胶焊接头的焊接强度与点焊接头的不同, 焊后直接对胶焊试样进行拉伸试验, 取消了胶层固化工艺. 拉伸试验下的胶焊接头如图 2 所示.

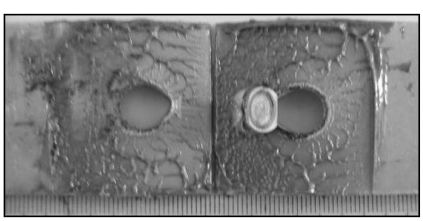

图 2 拉剪试验下的未固化胶焊接头搭接面

Fig. 2 Faying surface without cure under mechanical test

2 试验结果与对比分析

2.1 拉剪力对比

不同焊接时间下, 胶焊和点焊的焊点拉剪力与焊接电流的关系曲线见图 3. 在此, 拉剪力定义为试样在拉剪试验中的载荷—位移曲线所对应的峰值载荷. 当焊接电流不断增加时, 胶焊与点焊的焊点拉剪力均显著增加. 并且点焊拉剪力的增加速率要明显高于点焊.

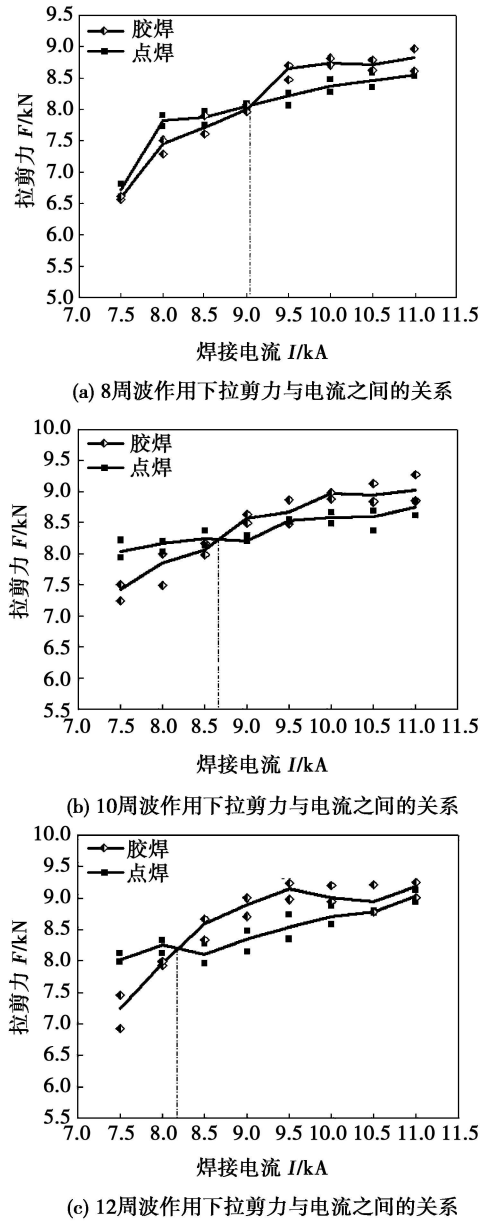

图 3 不同焊接时间和电流作用下胶焊和点焊的焊点拉剪力对比

Fig. 3 Comparison of tensile-shear force between weld-bonding and RSW under different welding time and current

从相同焊接工艺参数下的胶焊和点焊的拉剪力对比可看出, 在小电流情况下, 胶焊的拉剪力要普遍高于点焊, 且随着焊接时间的延长, 其差值有所增

加. 这是因为钢板搭接面上绝缘性的胶层阻碍了电极力作用下两钢板之间的接触面积，增加了焊接时的电流密度，使得胶焊在小电流情况下相对于点焊容易产生更多的热量，便于熔核的快速形成. 相反，在大电流情况下点焊的拉剪力比胶焊要高. 由于胶焊的热量积聚过于迅速，在中等电流情况下就已经会产生严重的焊接飞溅，破坏了熔核的生长. 而点焊要在更大的电流情况下才会发生一定程度的飞溅.

因此，在相同的焊接时间下，必然存在一个电流值使得胶焊与点焊的拉剪力恰好相等，即图 3 中交叉点对应的电流值. 此电流值是随着焊接时间的延长而逐渐减小的.

2.2　焊接性范围对比

依据上节胶焊、点焊工艺中的焊接电流和焊接时间与拉剪力的关系曲线，可分别确定以焊接电流与焊接时间为变量的 DP600 胶焊与点焊的焊接性范围，如图 4 所示. 其中，焊接性范围的左边界是以 8kN 拉剪力的等强度线为标准确定的，如果焊接参数的选择小于左边界，则焊点拉剪力达不到要求. 焊接性范围右边界是以产生飞溅为标准来确定的. 如果焊接参数的选择大于右边界，则认为飞溅程度过大，拉剪力将下降.

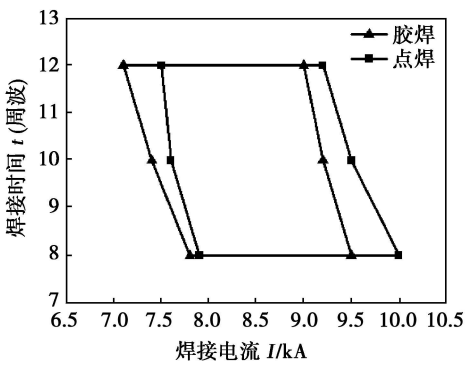

图 4　胶焊和点焊的焊接性范围对比

Fig. 4　Comparison of weld ability between weld-bonding and RSW

通过胶焊与点焊的焊接性范围对比可发现：一方面，胶焊的左边界要比点焊向左边偏移，即在小电流情况下，胶焊相对于点焊更易获得较大的焊点拉剪力；另一方面，胶焊的右边界亦向左偏移，即在较高的焊接电流下，胶焊更易产生飞溅现象.

2.3　焊接过程动态电阻曲线对比

胶焊和点焊焊点拉剪力的对比结果，可以通过其对应焊接过程中的动态电阻曲线进行分析阐述. 由图 5a 可见，由于不导电的胶层存在，使得胶焊在焊接初始阶段的电阻值要明显高于点焊，因此在小电流情况下胶焊焊接过程中的热量积聚较快，进而钢板的升温时间、局部熔化（熔核开始形成）时间要提前于点焊. 另一方面，当焊接电流较大时，如图 5b 所示，胶焊的热量非常大，在焊接的后半阶段，极易产生严重的飞溅，液态金属的喷溅导致焊点拉剪力的明显下降，最终，使得点焊的拉剪力反而会高于胶焊.

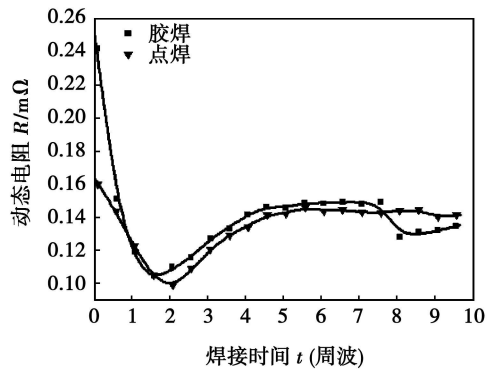

(a) 8 kA焊接电流作用下胶焊和点焊的动态电阻曲线对比图

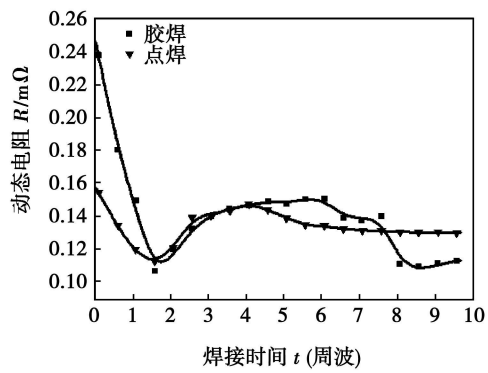

(b) 10 kA焊接电流作用下胶焊和点焊的动态电阻曲线对比图

图 5　10 周波作用下的胶焊和点焊动态电阻曲线对比图

Fig. 5　Comparison of dynamic resistance between weld-bonding and RSW under different welding current and time of 10 cycles

2.4　熔核微观组织对比

从小电流和大电流两种情况下胶焊和点焊焊点的熔核微观组织中可看出：在 8 kA 焊接电流下胶焊的熔核尺寸为 4.96 mm，而点焊熔核内部有气孔，且尺寸只有 4.33 mm，如图 6a，b 所示；在 10 kA 电流下胶焊的熔核尺寸与点焊熔核尺寸相当，达到 5.36 mm，如图 6c，d 所示. 但是由于 10 kA 电流下胶焊已经发生严重飞溅，熔核周围的部分胶和金属喷溅出来，且压痕较深，钢板变薄，最终使得点焊的接头强度反而高于胶焊接头.

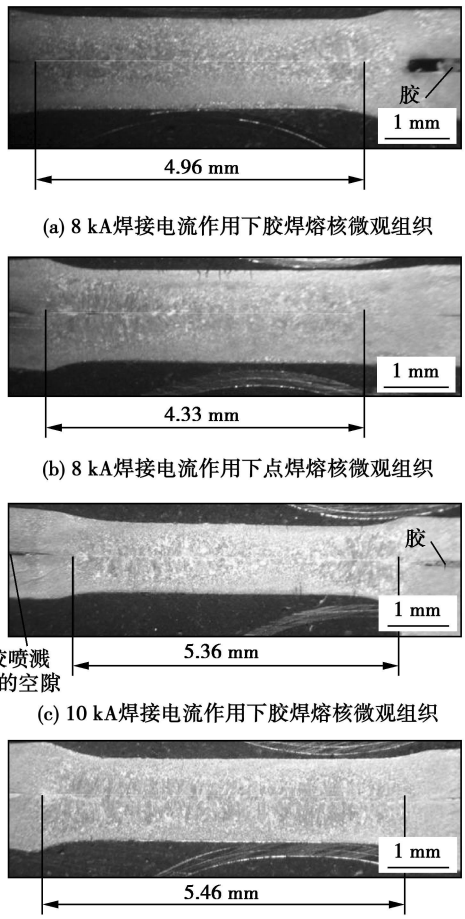

图 6 不同焊接电流下胶焊和点焊熔核微观组织对比

Fig. 6 Comparison of microstructure of nugget between weld-bonding and RSW under different welding current

3 结 论

(1) 由于胶焊焊接过程中的热量积聚较快, 熔核开始形成时间提前于点焊, 使得在小电流情况下胶焊的焊点拉剪力要普遍高于点焊.

(2) 由于胶焊的热量积聚过于迅速, 在中等电流情况下就已经会产生严重的焊接飞溅, 破坏了熔核的生长, 而点焊要在更大的电流情况下才会发生一定程度的飞溅. 使得在大电流情况下点焊焊点拉剪力要更高些.

(3) 在制定胶焊的焊接工艺参数时应选择比电阻点焊偏低的焊接电流, 而适度增加预压阶段的电极力能有效降低钢板间接触电阻, 保证焊接质量稳定, 而增大焊接过程后半阶段的电极力, 则有利于抑制飞溅产生.

参考文献:

[1] Tumuluru M D. Resistance spot welding of coated high-strength dual-phase steels[J]. Welding Journal, 2006, 85(8): 31—37.

[2] Marya M, Gayden X Q. Development of requirements for resistance spot welding dual-phase (DP600) steels part 1—the causes of interfacial fracture[J]. Welding Journal, 2005, 84(11): 172—182.

[3] Yasuhiko M. State of the art in precoated steel sheet for automotive body materials in Japan[J]. The Iron and Steel Institute of Japan International, 1991, 31(1): 1—10.

[4] 常保华, 史耀武, 卢良清. 胶焊搭接接头的应力分布和疲劳行为研究[J]. 机械工程学报, 2002, 36(2): 106—110.
Chang Baohua, Shi Yaowu, Lu Liangqing. Studies on stress distribution and fatigue behavior of weldbonded lap shear joints[J]. Chinese Journal of Mechanical Engineering, 2000, 36(2): 106—110.

[5] Melander A, Larsson M, Stensio H, *et al*. Fatigue performance of weldbonded high strength sheet steels tested in arctic, room temperature and tropical environments[J]. International Journal of Adhesion and Adhesives, 2000, 20(5): 415—425.

[6] Darwish S, Ghanya A. Critical assessment of weld-bonded technologies [J]. Journal of Materials Processing Technology, 2000, 105(3): 221—229.

作者简介: 孙海涛, 男, 1980 年出生, 博士研究生. 主要研究汽车车身连接工艺(胶焊、点焊等)、质量控制及其在线检测. 发表论文 4 篇.

Email: sht080@sjtu.edu.cn

Comparison of joint performance between weld-bonding and resistance spot welding of dual-phase steel SUN Haitao, ZHANG Yansong, LAI Xinmin, CHEN Guanlong (Shanghai Key Laboratory of Digital Autobody Engineering, Shanghai Jiaotong University, Shanghai 200240, China). p 17—20

Abstract: The joint performances between weld-bonding and resistance spot welding (RSW) are compared by tensile-shear force of nuggets, microstructure of nuggets, dynamic resistance curves and weld lobes. Experimental results show that the tensile-shear force of weld-bonded nuggets is much higher than that of spot-welded nuggets when lower welding current is used; oppositely tensile-shear force of spot-welded nuggets is a little higher than that of weld-bonded nuggets when higher welding current is used, but severe spatter will occur. Therefore, lower welding current in weld-bonding of steel comparing with that of RSW and larger electrode force during welding will inhibit spatter.

Key words: weld-bonding; resistance spot welding; dual-phase steel; joint performance

Fuzzy synthetical evaluation of weld bead stability for pulse MAG welding prototyping MENG Fanjun[1], ZHU Sheng[2], DU Wenbo[2] (1. Department of Remanufacturing Engineering, The Academy of Armored Forces Engineering, Beijing 100072, China; 2. National Key Laboratory for Remanufacturing, The Academy of Armored Forces Engineering, Beijing 100072, China). p 21—24

Abstract: Hierarchy analytical theory combined with the experiment is employed to determine the weld bead stability synthesis evaluation weight coefficient of weld surface quality, weld reinforcement and weld width of weld bead. The membership degree tables of surface quality, weld reinforcement and weld width are created by fuzzy theory. The analytic hierarchy theory and the fuzzy mathematics are applied to evaluate practical bead stability. The results show that the calculation value accords with the actual result, which proves the method of bead stability evaluation is effective.

Key words: weld bead stability; hierarchy analytical theory; fuzzy evaluation

Fatigue failure analysis of 6N01-T5 aluminum alloy welded joints LIU Xuesong[1], LI Shuqi[1], WANG Ping[1], MENG Lichun[2], LÜ Renyuan[2] (1. State Key Laboratory of Advanced Welding & Joining, Harbin Institute of Technology, Harbin 150001, China; 2. CSR Sifang Locomotive and Rolling Stock, Co. Lt, Qingdao 266000, China). p 25—28

Abstract: To identify the main cause of fatigue failures of welded joints of 6N01-T5 aluminum alloy extrusions, fatigue tests were carried out upon 6N01-T5 aluminum alloy extrusions and their weld joints, and S-N curves and conditional fatigue limits of them were obtained. Microstructure and mechanical properties of the welded joints were investigated. The fatigue fractures of the joints were analyzed and thereby the characteristics of them were obtained. The results show that the microscopic structure of the joints is α-Al and pseudo eutectic made up of α-Al and Mg_2Si; the defects of the joints are mainly gas cavities; there is a soften zone between HAZ and base metal which lead to fracture under dead-load but hardly to fracture failure; the main influence factors of fatigue performance are defects on the surface of weld and the surface condition of the weldment.

Key words: 6N01-T5 aluminum alloy; welded joints; S-N curve; fatigue failure

Corrosion resistance of intermediate temperature filler metal for stepped welding to 6063 aluminum alloy ZHU Hong[1,2], XUE Songbai[1], SHENG Zhong[1] (1. College of Materials Science and Technology, Nanjing University of Aeronautics and Astronautics, Nanjing 210016, China; 2. 14th Research Institute, China Electronic Technology Group Corporation, Nanjing 210013, China). p 29—32

Abstract: The effects of contents of Si, Cu, Ni and RE on the corrosion potential, weightlessness and corrosion rate of Al-Si-Cu-Ni-RE filler metal were studied by using orthogonal test, and the microstructure of the corroded filler metal was analyzed by means of SEM and EDS. It is indicated that the corrosion potential of the filler metal is relative to its weightlessness, which with the increase of the negative value of corrosion potential, the weightlessness increases continuously. Based on the corrosion rates, the results show that Ni has the most important influence on the melting points, and then do Si, Cu and RE. Through observed and analyzed the microstructure of filler metal, it is found that the matrix phase α (Al) with face-centered cubic solid solution makes the performance of joint better, but black brittle phase θ (Al_2Cu) makes the performance of joint poorer; Cl^- is the prime cause of induced pitting corrosion of the filler metal, which the pitting corrosion in filler metal and the obvious inter-granular corrosion are found in local area after corrosion.

Key words: orthogonal test; corrosion rate; pitting; inter-granular corrosion

Microstructure of magnesium alloy joints in resistance spot welding LANG Bo[1], SUN Daqian[2], REN Zhenan[2], ZHU Baiqing[3] (1. Beijing Aeronautical Manufacturing Technology Research Institute, Beijing 100024, China; 2. School of Materials Science and Engineering, Jilin University, Changchun 130025, China; 3. Beiqi Foton Motor Co., Ltd, Beijing 102206, China). p 33—36, 40

Abstract: The microstructure and phase composition of magnesium alloy joints in resistance spot welding are investigated with optical microscopy, confocal laser scanning microscope and X-ray diffraction for improving mechanical properties of the joints. The results show that the joints consist mainly of weld nugget and heat-affected zone (HAZ). The weld nugget contains two different structures, the cellular-dendritic structure at the edge of the nugget and the equiaxed dendritic structure in the center of the nugget. The weld nugget consists of α-Mg phase and a small amount of β-$Mg_{17}Al_{12}$ phase. Comparing with the grains in no melting base metal, the